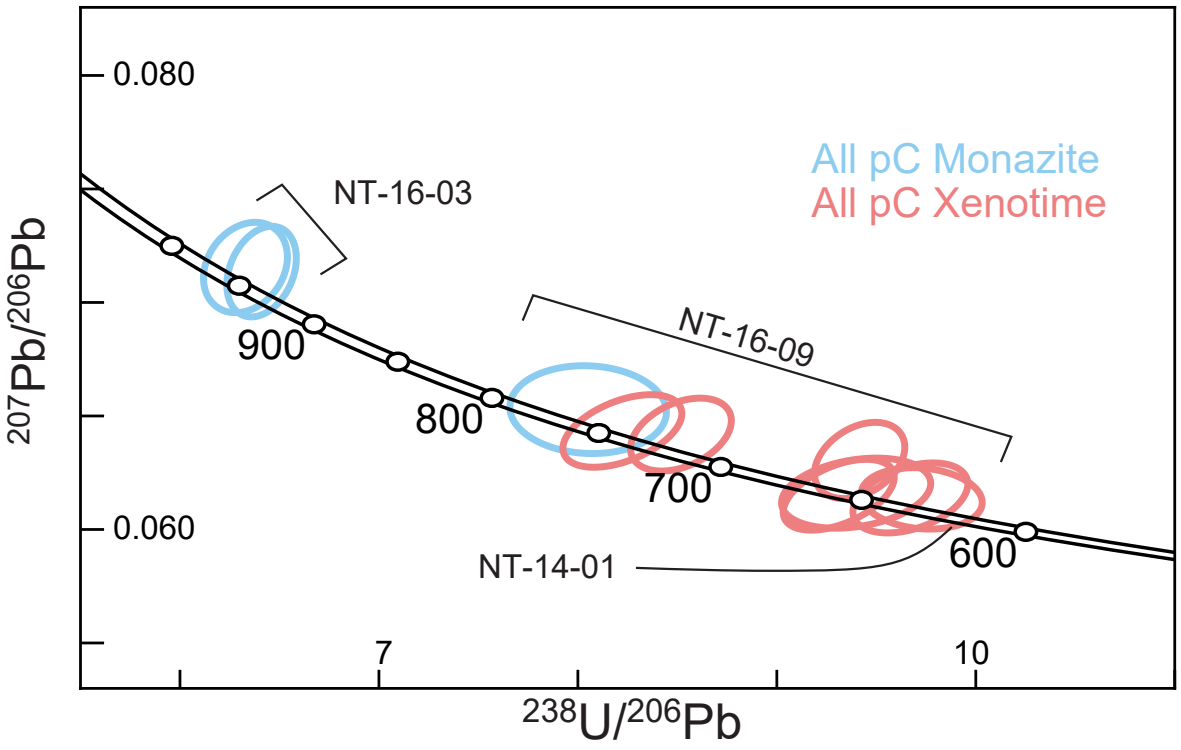

Supplementary Figure 1: Terra-Waserburg diagram showing data from monazite (blue) and xenotime (red) older than 500 Ma. These data may relate to older metamorphic events such as the the Knoydartian orogeny. 930-940 Ma monazite (included in garnet) may be detrital in origin.

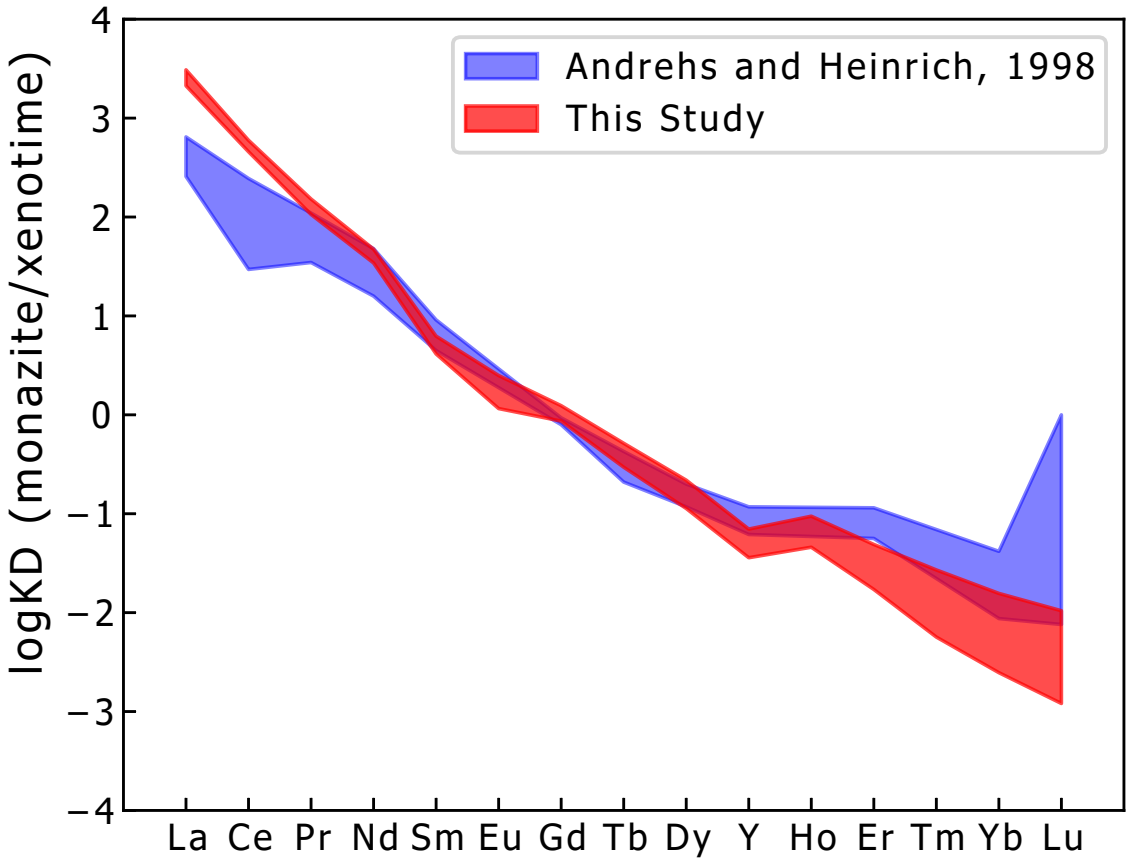

Supplementary Figure 2: A comparison of REE partitioning in monazite and xenotime from this study and that of Andrehs and Heinrich (1998). The range of our data mostly overlaps with the experimental data of Andrehs and Heinrich (1998). The general match can be regarded as an indicator of equilibrium between monazite and xenotime, so greater confidence can be placed in the constraints from monazite-xenotime thermometry.

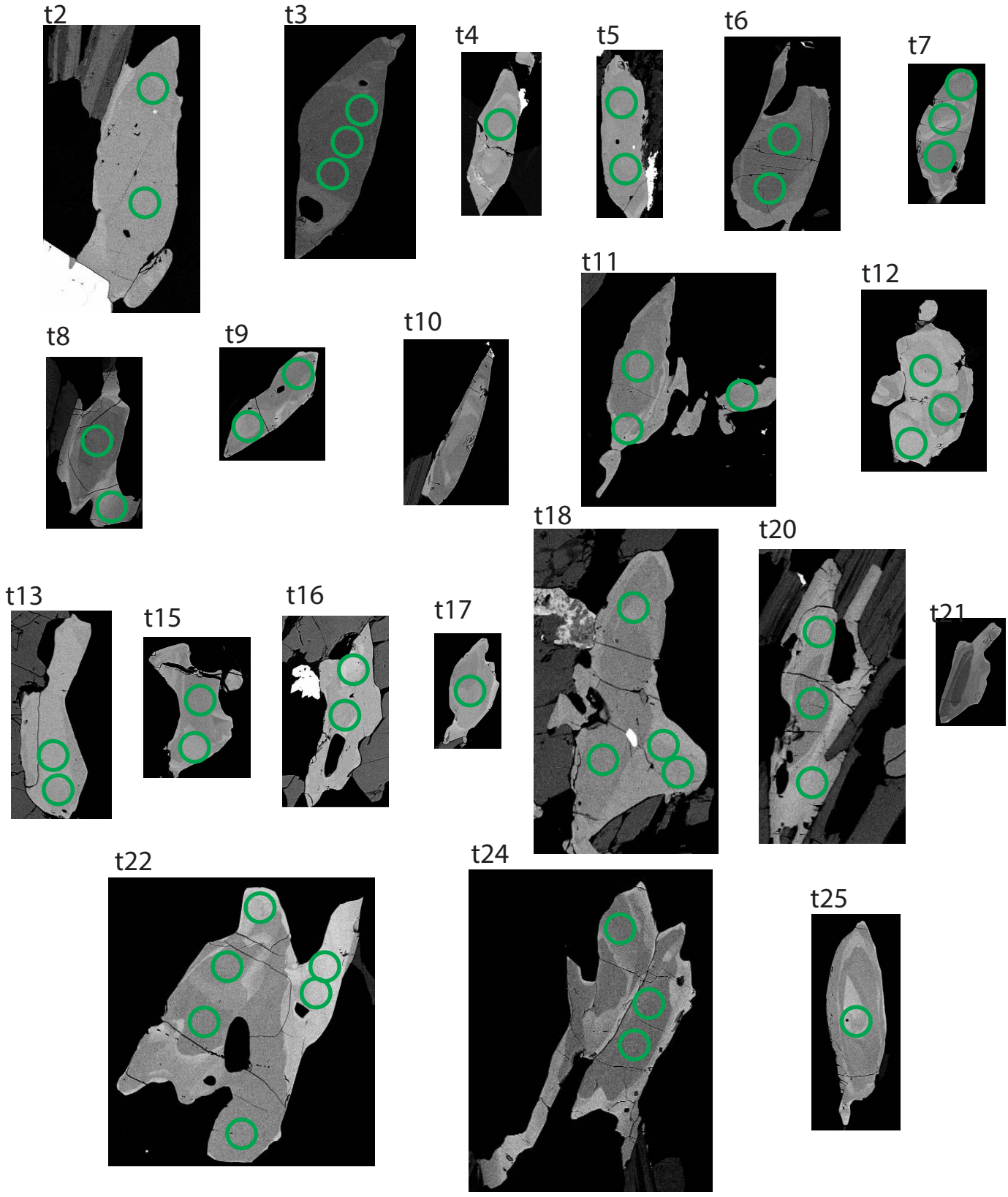

Supplementary Figure 3: Backscatter electron images of titanite with locations of laser ablation spots. These can be associated with isotopic and trace element data using x-y coordinates of titanite spots listed in supplementary table 2.

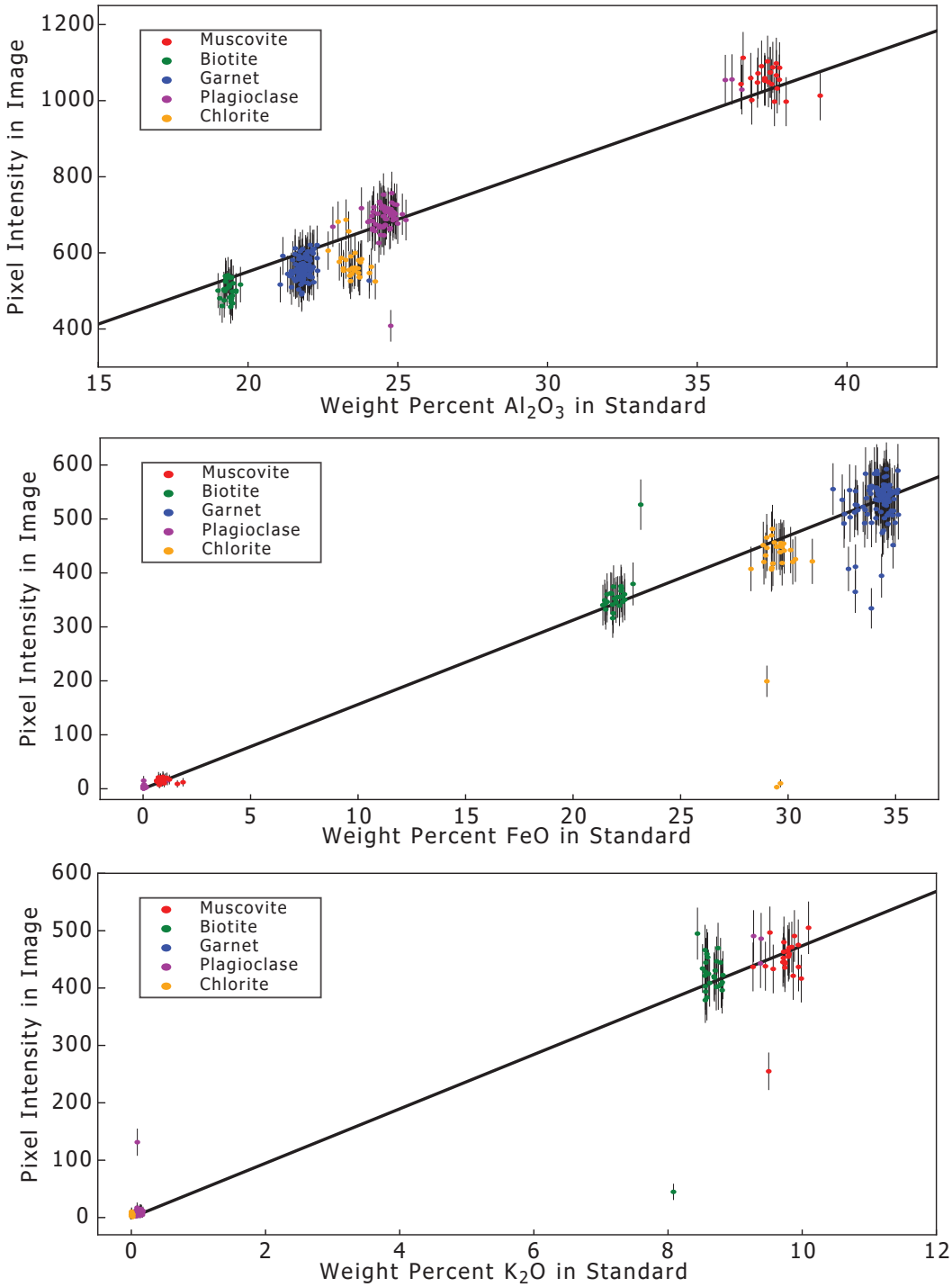

Supplementary Figure 4: Calibration of x-ray images using XMapTools (Lanari et al., 2014). The relationship between EPMA-measured composition and pixel intensity (counts per second) in an x-ray image of the same area is used to calculate the composition of the whole image area. These calibrations were used to calculate the compositions of course-grained muscovite in sample NT-04 (NT-14-01), which was not measured by EPMA, but was capture in x-ray images. We used EPMA data from all mineral phases to construct the calibration. This approach appears to give much more reasonable muscovite compositions than are obtained from a calibration using only muscovite EPMA analyes.

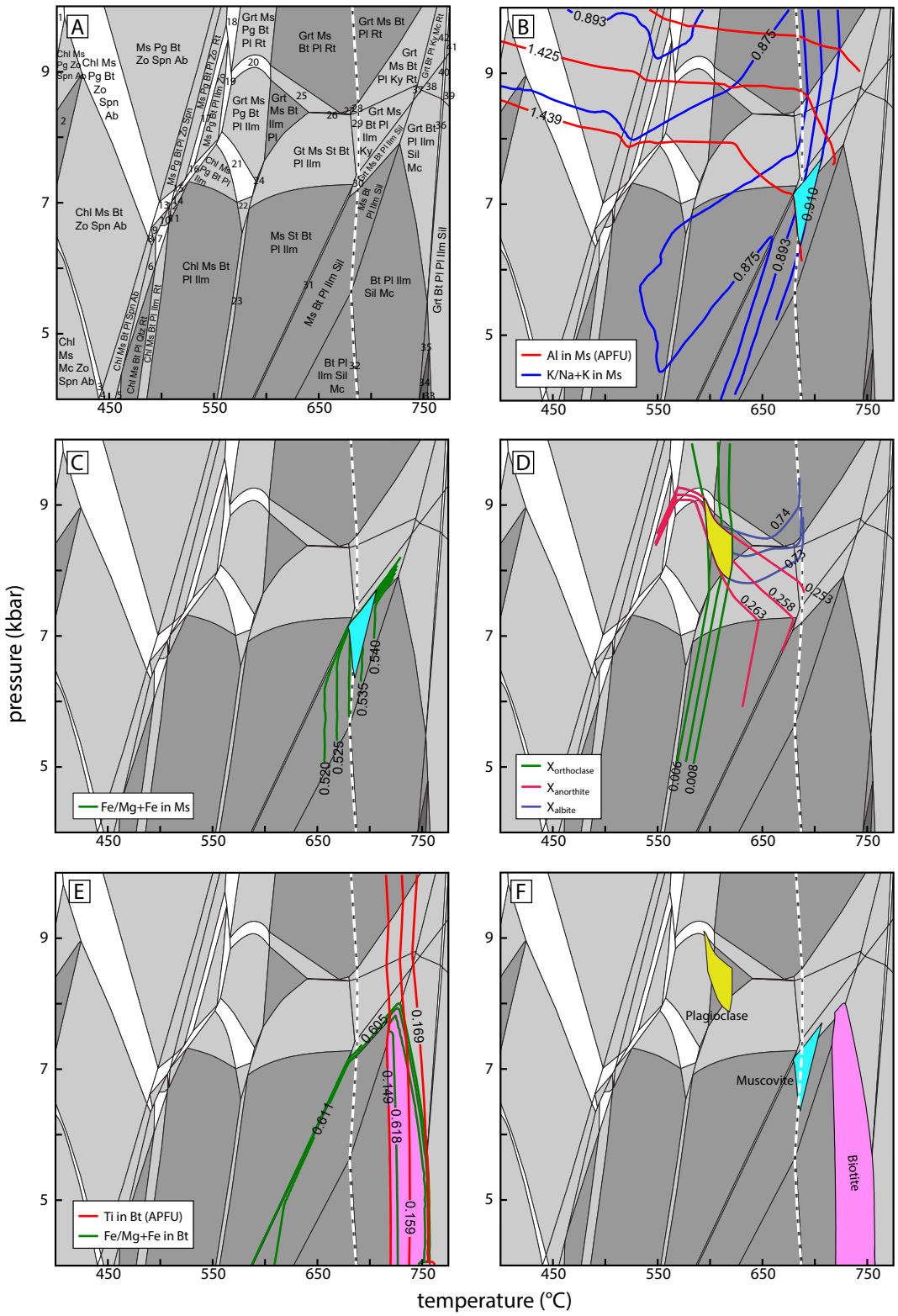

Assemblage (+Qz, +H2O)
1: Chl Ms Pg Zo Spn Fe-Stp Ab
2: Chl Ms Zo Spn Ab
3: Chl Ms Bt Zo Spn Ab Mc
4: Chl Ms Bt Pl Ab Rt
5: Chl Ms Bt Pl Spn Ab Mc
6: Chl Ms Bt Pl Spn Rt
7: Chl Ms Bt Pl Ilm Spn Rt
8: Chl Ms Pg Bt Pl Spn Ab
9: Chl Ms Pg Bt Pl Spn
10: Chl Ms Bt Pl Ilm Spn
11: Chl Ms Bt Pl Ilm Zo Rt
12: Chl Ms Bt Pl Ilm Zo Spn
13: Chl Ms Pg Bt Pl Zo Spn
14: Chl Ms Bt Pl Ilm Zo
15: Chl Ms Pg Bt Pl Zo Rt
16: Chl Ms Pg Bt Pl Ilm Zo
17: Ms Pg Bt Pl Ilm Zo Rt
18: Grt Ms Pg Bt Pl Zo Rt
19: Grt Ms Pg Bt Pl Ilm Zo
20: Grt Ms Pg Bt Pl Ilm Rt
21: Chl Grt Ms Pg Bt Pl Ilm
22: Chl Grt Ms Bt Pl Ilm
23: Chl Ms St Bt Pl Ilm
24: Grt Ms Pg St Bt Pl Ilm
25: Grt Ms Bt Pl Ilm Rt
26: Grt Ms St Bt Pl Ilm Rt
27: Grt Ms St Bt Pl Rt
28: Grt Ms Bt Pl Ky Rt
29: Grt Ms Bt Pl Ilm Ky
30: Grt Ms Bt Pl Ilm Sil
31: Ms St Bt Pl Ilm Sil

Assemblage (+Lq, +Qz)
32: Bt Pl Ilm Sil Mc H2O
33: Bt Pl Ilm Sil
34: Grt Bt Pl Ilm Si
35: Bt Pl Pl Ilm Sil
36: Grt Bt Pl Pl Ilm Sil Mc
37: Grt Bt Pl Ilm Ky Mc
38: Grt Bt Pl Sil Mc Rt
39: Grt Bt Pl Pl Sil Rt
40: Grt Bt Pl Pl Sil Mc Rt
41: Grt Bt Pl Pl Ky Rt
42: Grt Bt Pl Pl Ky Mc Rt

Supplementary Figure 5: P-T phase diagram and constraints on the conditions of plagioclase, muscovite and biotite equilibration. A) Labeled assemblage fields calculated from the composition of sample NT-04 (NT-14-01). The numbered fields refer to the list of assemblages above and to the right. B) P-T conditions of calculated (XMapTools) muscovite Al and K compositions at equilibrium. The positions of these isopleths in P-T space are based on the low water content equilibrium thermodynamic model. C) P-T conditions of the Fe composition (XMapTools) of muscovite at equilibrium. D) Equilibrium conditions of low-Ca plagioclase core compositions. E) Equilibrium conditions for biotite Fe# and Ti compositions. F) Summary of P- T conditions for plagioclase, muscovite and biotite equilibration. All of the isopleths shown here were smoothed using a Gaussian filter.

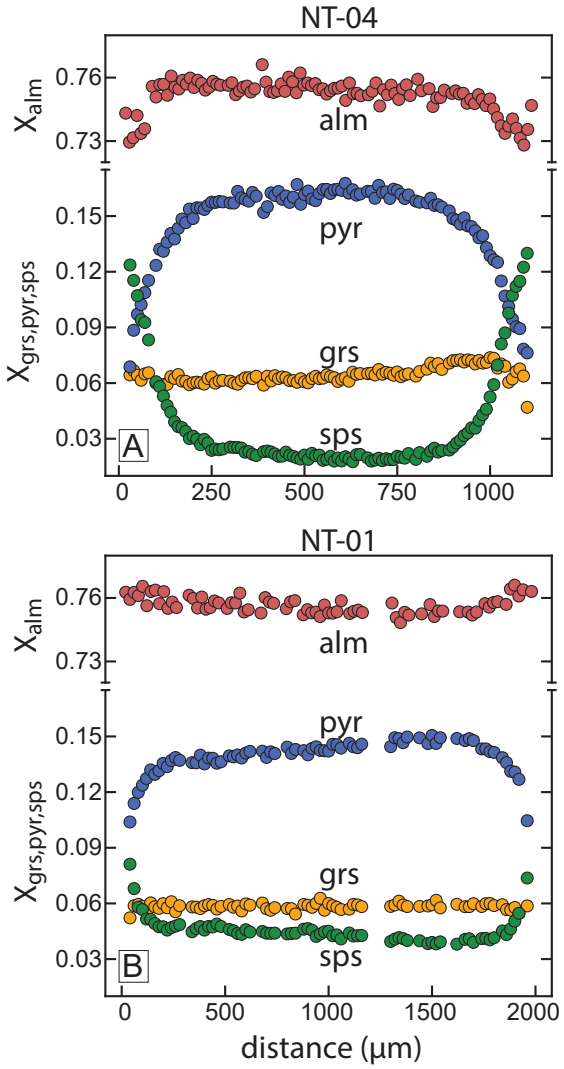

Supplementary Figure 6: Compositional traverses across garnets in samples A) NT-04 and B) NT-01. We interpret the relatively uniform core compositions to indicate significant diffusional modification of original compositional zoning, making the use of garnet compositions in P-T constraints inappropriate.

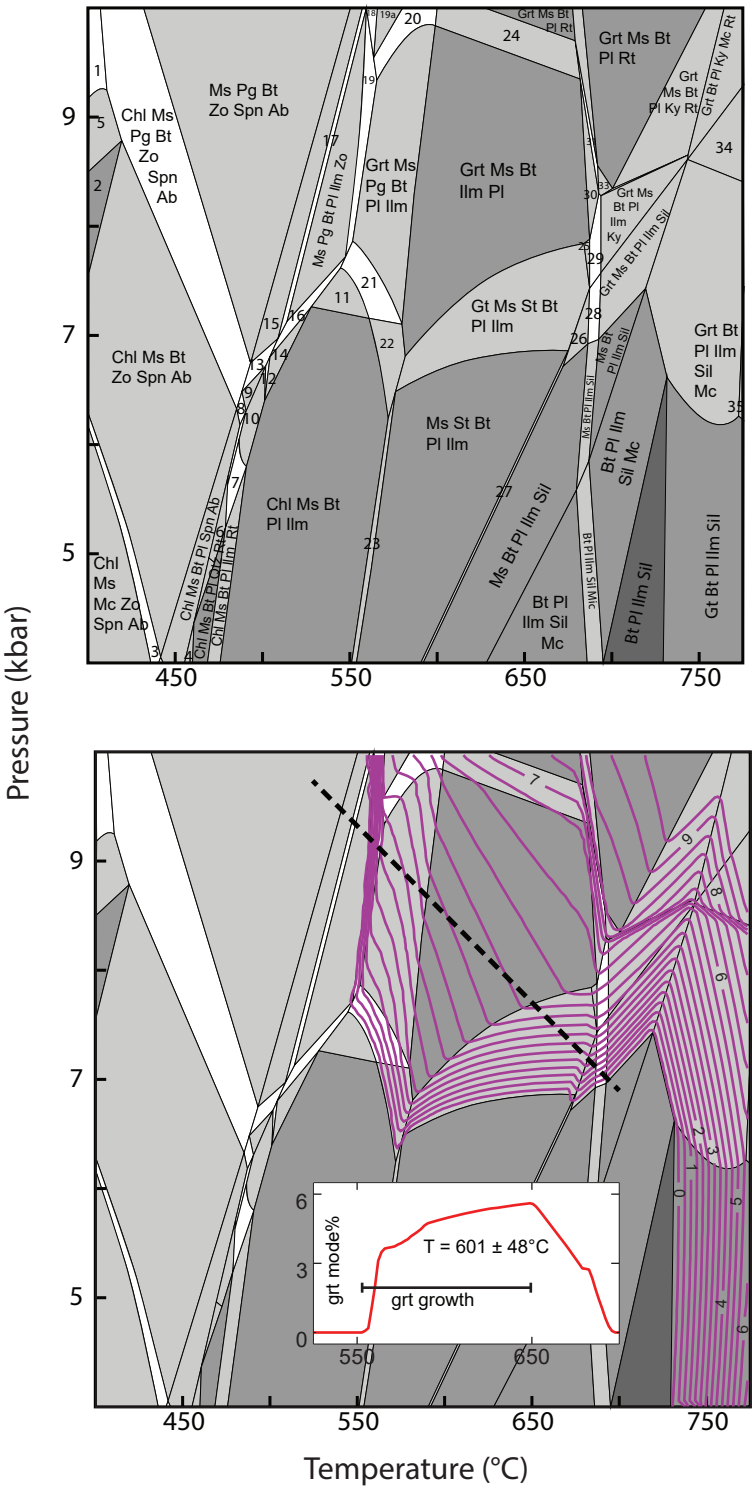

Assemblage (+Qz, +H2O)
1: Chl Ms Pg Zo Spn Fe-Stp Ab
2: Chl Ms Bt Zo Spn Ab
3: Chl Ms Bt Zo Spn Ab Mc
4: Chl Ms Bt Pl Ab Rt
5: Chl Ms Pg Bt Zo Spn Ab
6: Chl Ms Bt Pl Spn Rt
7: Chl Ms Bt Pl Ilm Spn Rt
8: Chl Ms Pg Bt Pl Spn Ab
9: Chl Ms Pg Bt Pl Spn
10: Chl Ms Bt Pl Ilm Spn
11: Chl Ms Pg Bt Pl Ilm
12: Chl Ms Bt Pl Ilm Zo Spn
13: Chl Ms Pg Bt Pl Zo Spn
14: Chl Ms Bt Pl Ilm Zo
15: Ms Pg Bt Pl Zo Spn
16: Chl Ms Pg Bt Pl Ilm Zo
17: Ms Pg Bt Pl Ilm Zo Rt
18: Grt Ms Pg Bt Pl Zo Rt
19: Grt Ms Pg Bt Pl Ilm Zo
19a: Grt Ms Pg Bt Pl Rt
20: Grt Ms Pg Bt Pl Ilm Rt
21: Chl Grt Ms Pg Bt Pl Ilm
22: Chl Grt Ms Bt Pl Ilm
23: Chl Ms St Bt Pl Ilm
24: Grt Ms Bt Pl Ilm Rt
25: Grt Ms Bt Pl Ilm Ky
26: Grt Ms Bt Pl Ilm Sil
27: Ms St Bt Pl Ilm Sil

Assemblage (+H2O, +Melt, +Qz)
28: Grt Ms Bt Pl Ilm Sil
29: Grt Ms Bt Pl Ilm Ky
30: Grt Ms Bt Pl Ilm
31: Grt Ms Bt Pl Ilm Rt
32: Grt Ms Bt Pl Rt

Assemblage (+Melt, +Qz)
33: Grt Ms Bt Pl Ilm Rt
34: Grt Bt Pl Sil Mc Rt
35: Grt Bt Pl Pl Ilm Sil

Supplementary Figure 7: P-T phase diagram for sample NT-01. Numbered assemblage fields are refer to the list at right. In the lower diagram, the purple contours reflect the modal proportion of garnet at equilibrium. The inset graph shows the modal proportion of garnet along the proposed P-T for sample NT-04 (~10 km along strike). Garnet mode is increasing from 553 to 649°C, so this temperature range is associated with the growth of low Y garnet domains in this sample.

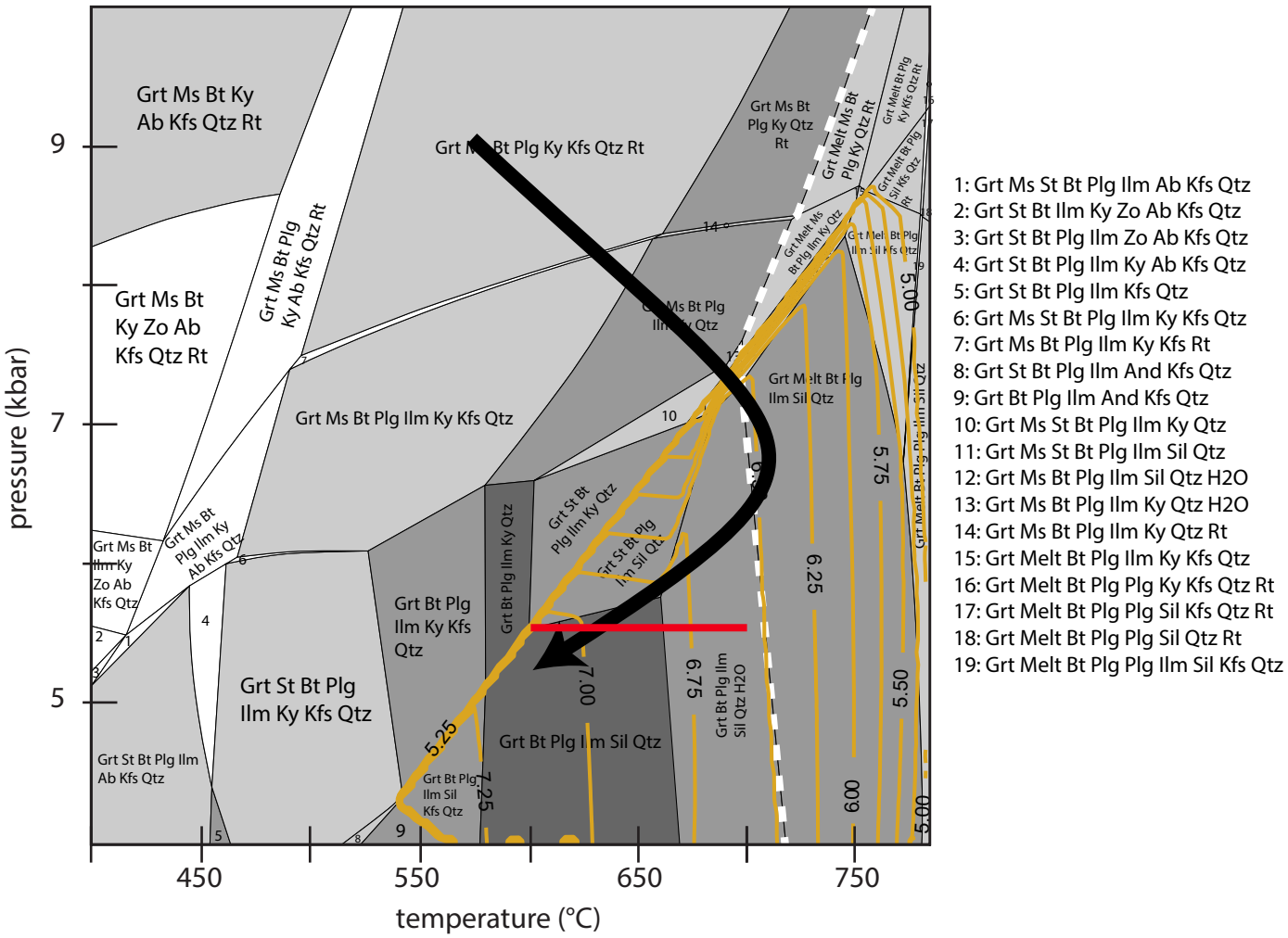

1: Grt Ms St Bt Plg Ilm Ab Kfs Qtz
2: Grt St Bt Ilm Ky Zo Ab Kfs Qtz
3: Grt St Bt Plg Ilm Zo Ab Kfs Qtz
4: Grt St Bt Plg Ilm Ky Ab Kfs Qtz
5: Grt St Bt Plg Ilm Kfs Qtz
6: Grt Ms St Bt Plg Ilm Ky Kfs Qtz
7: Grt Ms Bt Plg Ilm Ky Kfs Rt
8: Grt St Bt Plg Ilm And Kfs Qtz
9: Grt Bt Plg Ilm And Kfs Qtz
10: Grt Ms St Bt Plg Ilm Ky Qtz
11: Grt Ms St Bt Plg Ilm Sil Qtz
12: Grt Ms Bt Plg Ilm Sil Qtz H2O
13: Grt Ms Bt Plg Ilm Ky Qtz H2O
14: Grt Ms Bt Plg Ilm Ky Qtz Rt
15: Grt Melt Bt Plg Ilm Ky Kfs Qtz
16: Grt Melt Bt Plg Plg Ky Kfs Qtz Rt
17: Grt Melt Bt Plg Plg Sil Kfs Qtz Rt
18: Grt Melt Bt Plg Plg Sil Qtz Rt
19: Grt Melt Bt Plg Plg Ilm Sil Kfs Qtz

Supplementary Figure 8: P-T phase diagram for sample NT-03 (NT-16-09). This thermodynamic model was calculated with low water contents (H2O = 1 wt%), which likely provides a better match with peak to retrograde conditions. Orange contours represent the modal proportion of sillimanite at equilibrium. The large back arrow shows the proposed P-T path for sample NT-04 (~300m away). Sample NT-03 exhibits large amounts of sillimanite commonly intergrown with biotite. The red bar represents the range of temperature conditions (650±50°C) where the modal proportion of sillimanite is similar to that seen in thin section and the proposed P-T path would result in sillimanite growth. We associate this temperature range with the age of monazite cores in this sample.